Current Problems in Diagnostic Radiology 51 (2022) 747–758

Current Problems in Diagnostic Radiology

journal homepage: www.cpdrjournal.com

The Forgotten Phacomatoses: A Neuroimaging Review of Rare Neurocutaneous Disorders

Amjad Samara, MD[a,*], Mariya Gusman, MD[b], Loai Aker, MD[c], Matthew S. Parsons, MD[b], Ali Y. Mian, MD[b], Rami W. Eldaya, MD, MBA[b]

[a] Department of Psychiatry, Washington University School of Medicine, St. Louis, MO.
[b] Mallinckrodt Institute of Radiology, Washington University School of Medicine, St. Louis, MO.
[c] Department of Radiology, Hamad General Hospital, Doha, Qatar.

A B S T R A C T

Phakomatoses, or neurocutaneous syndromes, are a heterogeneous group of rare genetic disorders that predominantly affect structures arising from the embryonic ectoderm, namely the skin, eye globe, retina, tooth enamel, and central nervous system. Other organs are also involved in some syndromes, mainly cardiovascular, pulmonary, renal, and musculoskeletal systems. Currently, more than sixty distinct entities belonging to this category have been described in the literature. Common phakomatoses include conditions like Neurofibromatosis and Tuberous sclerosis. Several review papers have focused on various aspects of these common conditions, including clinical presentation, genetic and molecular basis, and neuroimaging features. In this review, we focus on rare neurocutaneous syndromes: Melanophakomatoses (Ie, Neurocutaneous Melanosis, and Incontinentia Pigmenti), Vascular Phakomatoses (Ie, Ataxia Telangiectasia and PHACE Syndrome), and other conditions such as Cowden Syndrome, Basal Nevus Syndrome, Schwannomatosis, Progressive Facial Hemiatrophy, Gomez-Lopez-Hernandez Syndrome, Wyburn-Mason Syndrome, CHILD Syndrome, and Proteus Syndrome. We also review the neuroradiologic manifestations of these conditions as a guide for neurologists and neuroradiologists in their daily practice.

Introduction

The phakomatoses, or neurocutaneous syndromes, are a heterogeneous group of disorders characterized by multiple congenital anomalies affecting the eye, skin, and central nervous systems (CNS).[1] Other organ systems can be affected, including cardiovascular, pulmonary, renal, and musculoskeletal systems. The most frequently discussed phakomatoses like neurofibromatosis type 1 (NF-1) and type 2 (NF-2), tuberous sclerosis, Sturge-weber, and von Hippel-Lindau syndrome have received significant attention in the medical literature with several recent reviews.[2] However, we identified a group of uncommon phakomatoses that have received less attention and can challenge physicians unfamiliar with their imaging manifestations. With the recent advancements in genetic and molecular diagnostic tools and neuroimaging modalities, more than 60 neurocutaneous conditions with various phenotypes have been reported.[1,3] A recent review proposed a new classification system that divides phakomatoses into 6 subgroups based on clinical phenotype.[1] These subgroups are: (1) *predisposing to the development of tumors* (Ie, neurofibromatosis, tuberous sclerosis, schwannomatosis, and Cowden syndrome); (2) *with vascular malformations* (Ie, Sturge-weber and Klippel-Trenaunay-Weber syndromes, Hereditary Hemorrhagic Telangiectasia, Wyburn-Mason syndrome, and Blue rubber bleb syndrome); (3) *with vascular tumors* (Ie, Von Hippel-Lindau syndrome, and PHACE syndrome); (4) *with pigmentary/connective tissue mosaicism* (Eg, Hypomelanosis of Ito, Incontinentia pigmenti, and Neurocutaneous melanosis); (5) *with dermal dysplasia* (Eg, cerebellotrigeminal dermal dysplasia); and (6) *with twin spotting or similar phenomena* (Eg, phacomatosis pigmentovascularis).

Imaging studies are essential in evaluating phakomatoses and screening children presenting with suspicious skin or eye manifestations, especially magnetic resonance imaging (MRI). The goal of this paper is not an exhaustive review of neurocutaneous disorders, rather a summary of relevant clinical and neuroradiologic features of selected rare entities; those we felt would be high yield to neurologists and neuroradiologists given they are underrepresented in the literature.

Melanophakomatoses

Neurocutaneous Melanosis

Neurocutaneous Melanosis (NM; MIM # 249400) is a congenital disorder characterized by a combination of large or multiple

Abbreviations: AT, Ataxia telangiectasia; AVM, arteriovenous malformations; BCC, basal cell carcinoma; BNS, Basal nevus syndrome; CMN, Congenital melanocytic nevi; CNS, central nervous system; DVM, Developmental venous anomaly; GLHS, Gomez-Lopez-Hernández syndrome; IP, Incontinentia pigmenti; NBCCS, Nevoid basal cell carcinoma syndrome; NF-1, neurofibromatosis type 1; NF-2, neurofibromatosis type 2; NM, Neurocutaneous melanosis; PFH, Progressive facial Hemiatrophy

Funding: AS was supported by National Institute on Drug Abuse (grant number 5T32DA007261-29).

Conflict of interests: The authors declare that they have no competing interests.

*Reprint requests: Amjad Samara, MD, Department of Psychiatry, Washington University School of Medicine, 4525 Scott Ave, St. Louis, MO 63110.
E-mail address: amjadsamara09@gmail.com (A. Samara).

https://doi.org/10.1067/j.cpradiol.2021.07.002
0363-0188/

pigmented proliferations in the skin present at birth (congenital melanocytic nevi or CMN) plus benign or malignant tumors of the leptomeninges with CNS involvement.[4] The Congenital Melanocytic Nevi (CMN) frequency is about 1 in 20,000 to 500,000 live births with a female to male ratio of around 3:2.[5,6]

Genetics: NM has a sporadic pattern of inheritance. Kinsler et al. conducted a genetic analysis on 55 samples from 15 patients with CMN and suggested that CMN and neuromelanosis are caused by somatic mosaicism for *NRAS* gene mutations in neuroectodermal progenitor cells.[7] However, 3 of the original 15 patients did not exhibit *NRAS* mutation, suggesting an alternative, yet unknown, genetic cause. The authors also showed that loss of heterozygosity is associated with the timing of progression to malignancy, suggesting a multistep model of transformation.[7] *NRAS* gene, located on Chromosome 1p13.2, encodes for neuroblastoma RAS viral oncogene homologue (NRAS) protein, and abnormal NRAS protein inactivates cellular RAS signaling pathway.

Clinical presentation: NM diagnosis is based on clinical criteria with more than three congenital skin nevi OR giant congenital nevus ($>$ 20 cm in adults; $>$ 9 cm if infant head; or $>$ 6 cm, if infant trunk) and imaging findings of meningeal or CNS melanosis. The primary manifestations in most patients are CMN and proliferation of melanocytes in meninges and brain parenchyma. Giant CMNs are associated with an increased risk of the development of melanoma. Although most patients with CNS involvement are asymptomatic, some patients present with hydrocephalus and seizures (which may result from intracranial bleeding or impaired cerebrospinal fluid circulation) and cranial nerve dysfunction.[8] Helpful screening tools include MRI with gadolinium contrast enhancement and CSF cytology.

Neuroimaging: The 2 most common imaging findings are pachymeningeal and leptomeningeal melanosis.[9] Melanin is bright on T1 weighted MRI. Therefore, the presence of parenchymal, pachymeningeal, or leptomeningeal foci showing intrinsic T1 shortening is very suggestive of melanosis. The amygdalae are the most common locations for parenchymal melanocytic deposits. Less common sites include the brainstem, cerebellum, cerebral cortex, or thalamus. Leptomeningeal melanosis is more commonly distributed anteriorly and ventrally. Although these lesions are seen on T1 as hyperintensities, post-contrast MRI scans better show the extent of the melanosis with superimposed contrast enhancement. NM could also progress to malignant melanoma, which is a frequent cause of mortality in these patients. Among the differential diagnoses, primary CNS melanoma also develops in the leptomeninges and may present as leptomeningeal melanosis. Posterior fossa structural abnormalities are common, affecting about 10% of NM, most commonly as Dandy-Walker malformation,[10] followed by hydrocephalus.[11] Other manifestations include structural abnormalities of the cerebellum (like posterior fossa cysts), defects of the vertebrae or skull, and intraspinal lipomas.[12] Spinal involvement (Eg, syringomyelia or arachnoiditis) is seen in about 20% of the patients. An example of these findings is presented in Figure 1.

Incontinentia Pigmenti

Incontinentia pigmenti (IP; MIM #308300), also known as Bloch-Siemens-Sulzberger syndrome, is a rare X-linked disorder that affects the skin, hair, teeth, nails, eyes, and CNS. IP is usually lethal prenatally in males. IP primarily affects the skin with characteristic blistering extremity rash in infants that progresses to wart-like growths in

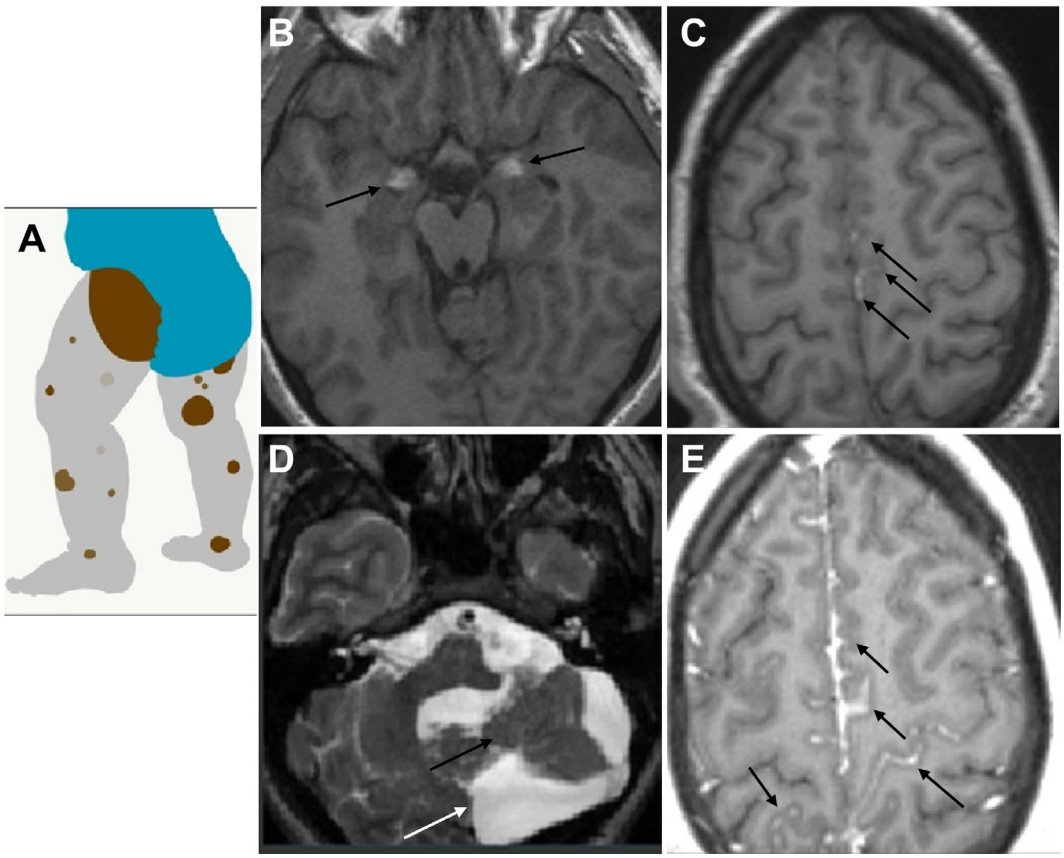

FIG 1. A 22-year-old patient with neurocutaneous melanosis. (A) Cartoon depicting cutaneous melanocytic nevi; (B) Axial T1WI non-contrast MRI demonstrating melanocytic deposit in the amygdala bilaterally (black arrows). (C) Axial T1WI non-contrast MRI shows melanocytic deposits along the meninges at the vertex (black arrows); (D) Axial T2WI demonstrates abnormal posterior fossa with cerebellar atrophy, cerebellar dysplasia (black arrow), and large CSF spaces/arachnoid cyst (white arrow). (E) Axial post-contrast T1WI shows extensive leptomeningeal enhancement consistent with more diffuse meningeal involvement. (Color version of figure is available online.)

children and swirled hyperpigmentation, and finally hypopigmentation. Histologically, melanin deposits are seen in the skin dermis, and the designated name “Incontinentia pigmenti” was based on the idea that the basal layer of the epidermis is 'incontinent' of melanin. Interestingly, skin lesions follow the so-called Blaschko lines, a distribution pattern that is a product of genetic mosaicism in the skin or mucosa and is common to several X-linked conditions. These lines trace the migration of embryonic cells and are generally distinct from the developmental margins formed by nervous, muscular, and lymphatic tissues.[13] Frequency of this condition is about 1 in 100,000-500,000 individuals.[14]

Genetics: IP is inherited in an X-linked dominant manner and caused by mutations in *IKBKG/NEMO* gene.[15] This gene encodes NEMO/IKKγ protein, which is required to activate the transcription factor nuclear factor−kappa B (NF−κB), protecting cells against TNF-α induced apoptosis. In most cases, loss-of-function mutations are detected.[16] Lack of this apoptosis inhibiting protein leads to abnormal cell death. About two-thirds of individuals have a *de novo* mutation. Genetic mutations are lethal in males, but some case studies report genetic mosaicism.[17] The IP diagnosis is based on clinical findings and can be confirmed by molecular genetic testing of the *IKBKG* gene.

Clinical presentation: In addition to skin involvement, other clinical signs of IP include alopecia, developmental absence of one or more teeth, abnormal tooth shape, and dystrophic nails. Neovascularization of the retina, present in some individuals, predisposes to retinal detachment.[18] Neurologic findings, including cognitive delays/intellectual disability, learning disability, and seizures, are occasionally seen.[19]

Neuroimaging: MRI is recommended in the assessment of newborn infants with IP. The role of imaging is to explain neurological deficits and as a secondary method to confirm the clinical suspicion. Imaging findings are only present in patients with neurologic disease associated with cutaneous lesions.[20] IP patients show signs of white matter abnormalities, multi-territorial infarcts, and small and medium vessel angiopathy. The majority of white matter lesions are oriented perpendicular to the corpus callosum, and hypoplasia of the corpus callosum is a common finding as well.[20] Diffusion-weighted imaging might show restricted diffusion in deep and subcortical white matter, thalami, basal ganglia, and cerebellum, indicating acute infarcts.[19] Magnetic resonance spectroscopy (MRS) might show metabolic changes in these infarct regions and the adjacent parenchyma, suggestive of glial proliferation and neuronal loss.[21,22] The underlying mechanisms of these imaging findings are unknown. Examples of the neuroradiological conclusions in IP are shown in Figure 2.

Vascular Phakomatoses

Ataxia Telangiectasia

Ataxia Telangiectasia (AT; MIM #208900), also known as Louis-Bar syndrome, is an autosomal recessive disorder that affects CNS, skin, eyes, and immune system. Specifically, AT is characterized by cerebellar ataxia, oculocutaneous telangiectasias, immune defects, and increased risk for malignancy. This rare genetic disease has an incidence of 1 in 40,000 to 100,000 individuals worldwide, and in the United States, about 1% of the population is a carrier of *ATM* gene mutation.[23]

Genetics: AT is caused by either homozygous or compound heterozygous mutation in the *ATM* gene. *ATM* gene is located on chromosome 11q22.3. ATM protein is involved in multiple cellular functions, particularly DNA repair and cell cycle control.[24] Cells with *ATM* gene mutations are susceptible to damage by ionizing radiation. Purkinje cells and granular cells of the cerebellar cortex are particularly sensitive, leading to prominent cerebellar atrophy.[25]

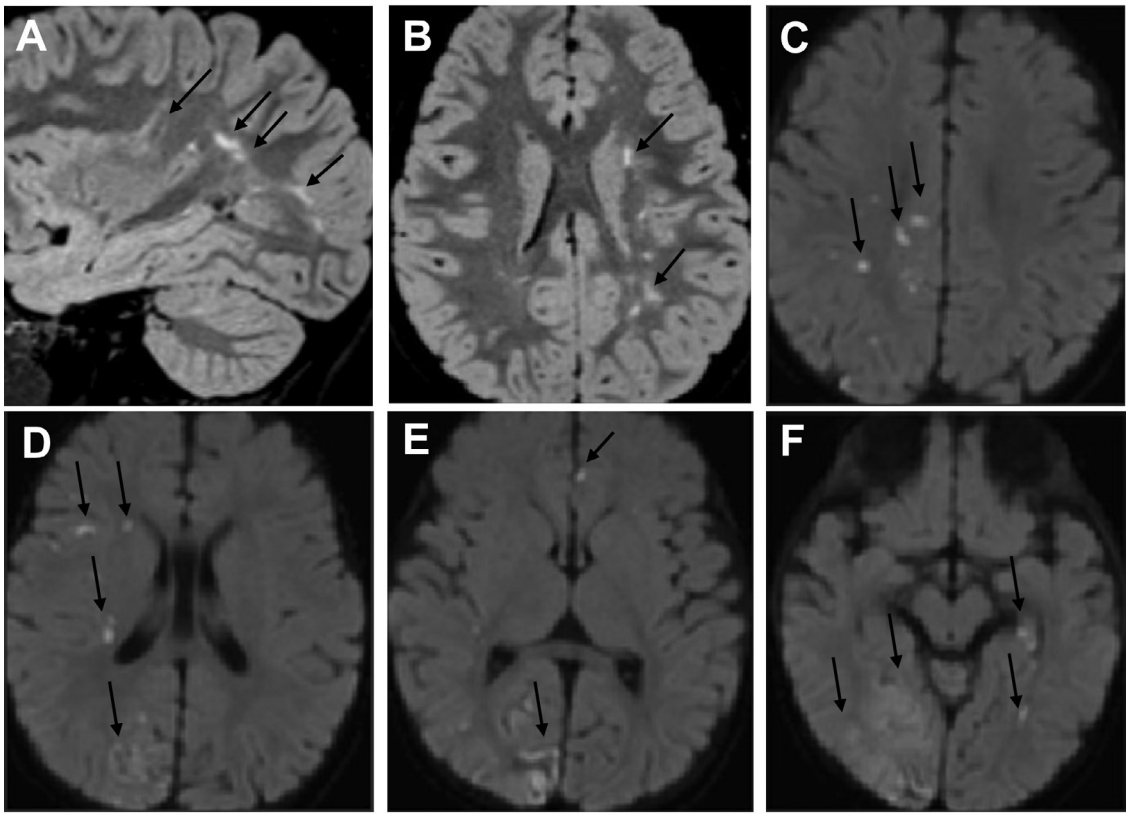

FIG 2. A 6-year-old patient with Incontinentia Pigmenti. (A) sagittal 3D FLAIR demonstrates multiple hyperintense white matter lesions (black arrows) reflective of chronic small vessel ischemic changes associated with Incontinentia Pigmenti. (B) axial 3D FLAIR shows multiple FLAIR hyperintense white matter lesions (black arrows) reflective of chronic small vessel ischemic changes associated with Incontinentia Pigmenti. (C-F) Axial DWI images from cranial (C) to caudal (F) demonstrate multifocal areas of DWI hyperintensity (black arrows) consistent with multiple territories of infarcts (ADC map not shown).

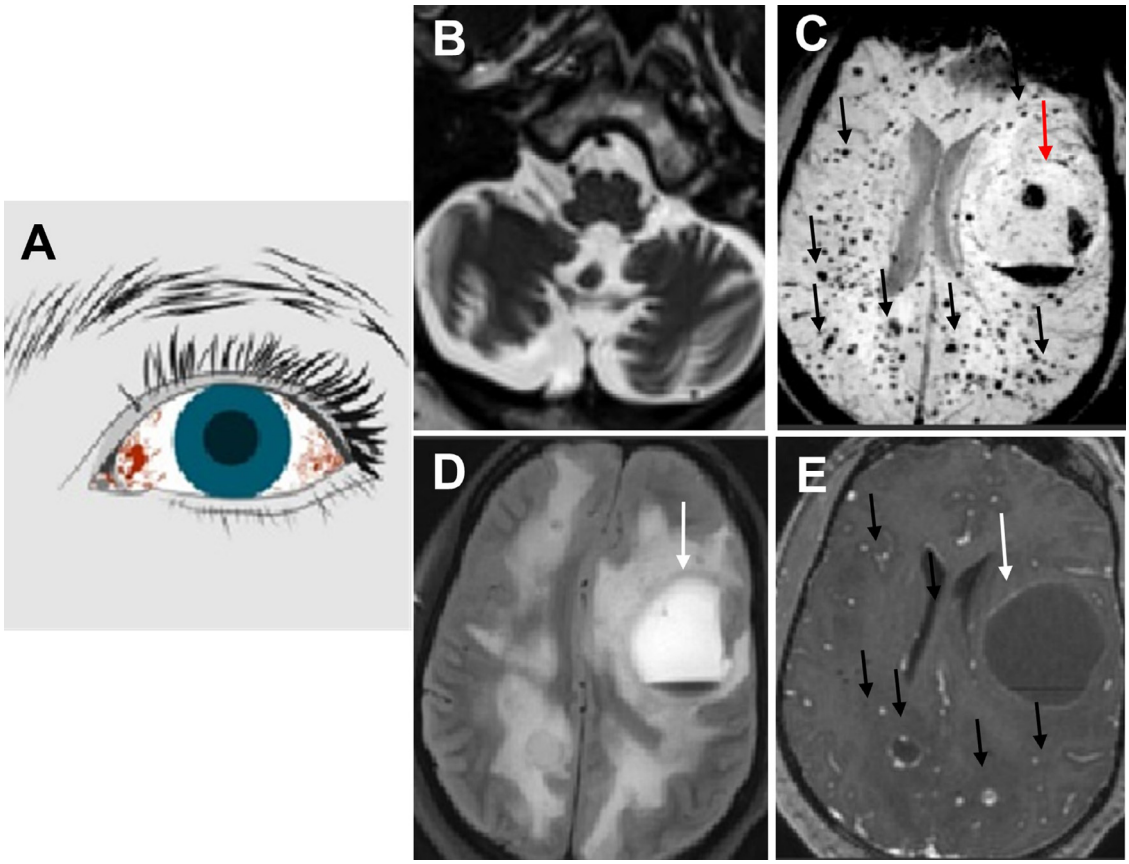

FIG 3. A 28-year-old patient with Ataxia Telangiectasia. (A) Cartoon depicting globe telangiectasia, a common finding in patients with Ataxia telangiectasia; (B) Axial T2WI at the level of the posterior fossa demonstrating extensive parenchymal volume loss advanced for age; (C) Axial SWI image demonstrates vast hemosiderin deposits (black arrows) reflective of telangiectasias/microhemorrhages. Also, a parenchymal hemorrhage appears as a fluid/blood level cystic lesion (red arrow), likely secondary to capillaries leak. (D) Axial FLAIR shows the parenchymal hemorrhage as a fluid collection (white arrow), likely secondary to capillaries leak, with confluent white matter hyperintensities thought to represent (but not confirmed) possible demyelination. (E) Axial post-contrast T1WI demonstrates foci of enhancement (black arrows) and thin rim enhancement (white arrow) surrounding the fluid collection that is likely secondary to telangiectasia and capillaries leak. (Color version of figure is available online.)

Clinical presentation: AT is a childhood-onset disease with symptoms seen as early as the first year of life. Motor neurologic symptoms start with gross motor skills and speech deterioration, followed by fine motor skills and eye coordination. Telangiectasias usually involve the eyes/conjunctiva, skin, and, less frequently, the brain.[26] AT patients also suffer from increased sensitivity to ionizing radiation, which increases the risk for neoplasms (Eg, leukemia). Diagnosis is established by genetic testing, but elevated α-fetoprotein levels (AFP) and CA-125 in regular lab workouts are suggestive of this condition.

Neuroimaging: In children, the most prominent imaging finding is cerebellar atrophy.[26] Cerebellar atrophy does not become apparent until 6 years of age. Pediatric AT patients often have no supratentorial findings. In contrast, adult patients tend to have telangiectasias, microhemorrhages, and occasionally space-occupying fluid collection, likely due to capillary leaks and cysts with peripheral or internal blood products.[26] AT patients over the age of 20 may develop extensive white matter T2/FLAIR signal abnormalities.[27] Both focal hemosiderin depositions and space-occupying lesions demonstrate surrounding enhancement, owing to prominent telangiectasias and increased capillary permeability. Susceptibility-weighted imaging commonly shows hypointense cerebral lesions that are supratentorial and predominantly lobar.[28] MRS shows signal abnormalities in the cerebellum of adults with AT that could be used to differentiate early stages of AT from other forms of ataxia and provide a marker for treatment efficacy monitoring.[29,30] An example of these findings is presented in Figure 3.

PHACE Syndrome

PHACE syndrome (MIM #606519) is a rare neurocutaneous disorder that usually involves dermatological, neurological, cardiovascular, and ocular abnormalities. PHACE acronym is based on the association of ***p***osterior fossa malformations, large facial ***h***emangiomas, cerebral ***a***rterial anomalies, ***c***ardiovascular anomalies, and ***e***ye anomalies.[31] PHACE(S) acronym is considered in the presence of ventral developmental abnormalities like sternal clefting or supraumbilical abdominal raphe.[32] While the overall incidence of PHACE syndrome is unknown, infantile hemangiomas have an estimated incidence of 4%-5% in all live births.[33] Also, a high female predominance was reported in PHACE patients.[34]

Genetics: The etiology of PHACE syndrome is not known. However, the high female predominance was suggestive of a potential X-linked dominant mutation with potential lethality in males.[32]

Clinical presentation: The hallmark of PHACE is the characteristic infantile facial hemangioma, typically segmental and large.[32] While the capillary malformations of Sturge–Weber syndrome are always conspicuous at birth and never regresses, PHACE infantile hemangiomas may not be visible at birth, usually demonstrating a rapid growth phase during the neonatal period, and tend to regress. Facial hemangiomas in PHACE do not follow a dermatomal distribution.[35] However, these hemangiomas can occur in one or more segmental patterns, unilaterally or bilaterally.[32] PHACE diagnosis is made when there is a segmental hemangioma or a facial or scalp hemangioma larger than 5 cm, plus two minor criteria or one major criterion.[32] Bayer et al. reported that 41% of 150 PHACE cases had cardiac, aortic arch, or brachiocephalic anomalies.[36] A spectrum of ophthalmologic

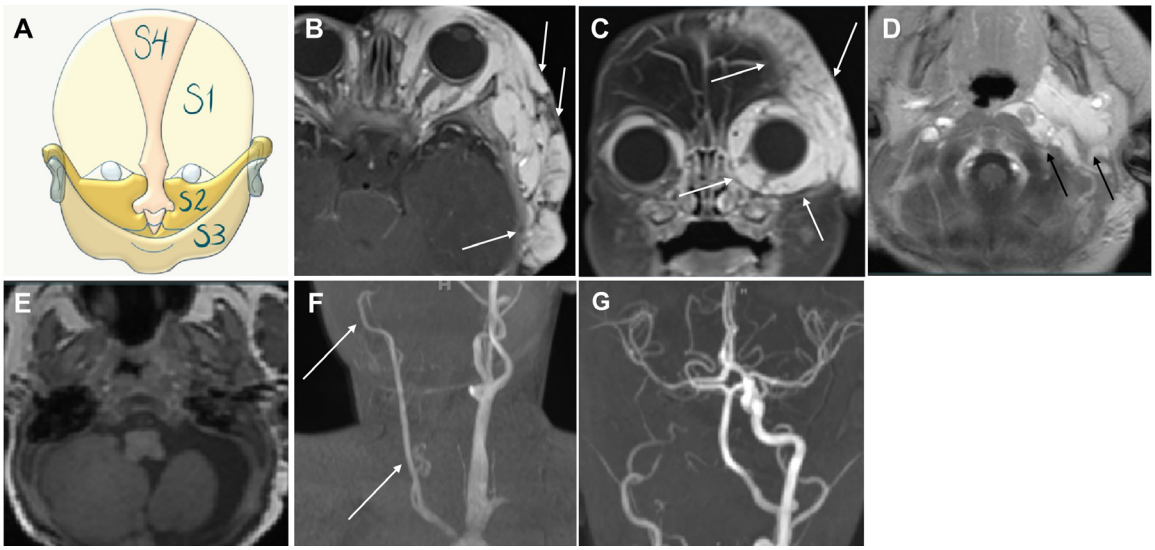

FIG 4. PHACE Syndrome. A cartoon depicting segmental hemangiomas segments (Segment 1, Frontotemporal; Segment 2, Maxillary Segment; 3, Mandibular Segment; 4, Frontonasal). (B-E): A 2-month old with segmental hemangioma and PHACE(s) syndrome. (B) Axial nonfat saturated post-contrast T1WI shows a left S1 segmental hemangioma (white arrows). (C) Coronal fat-saturated post-contrast T1WI shows S1 segmental hemangioma involving the orbit (white arrows). (D) Axial nonfat saturated post-contrast T1WI at the level of the suprahyoid neck shows a left-sided suprahyoid extension of the segmental hemangioma (black arrows). (E) Axial T1WI shows associated posterior fossa anomaly with hypoplastic left cerebellar hemisphere. 6(F-G): An 8-year-old with PHACE(S) syndrome. (F) Coronal neck MRA time-of-flight MIP demonstrates an absence of right cervical internal carotid artery and vertebral artery. Arrows depict the common carotid artery and external carotid artery. (F) Axial MRA time-of-flight MIP shows absent right internal carotid artery with a robust supply of the right anterior and middle cerebral arteries from collateral circulation. (Color version of figure is available online.)

abnormalities affecting anterior and posterior segments of the eye has been reported as well.[32]

Neuroimaging: Posterior fossa abnormalities in PHACE includes focal cerebellar lesions, cerebellar hypoplasia, posterior fossa arachnoid cysts, and Dandy-Walker complex.[32,37] The prevalence of posterior fossa abnormalities ranges between 30 and 81%.[31,32,38] The focal unilateral cerebral/cerebellar lesions tend to occur on the same side as the cutaneous hemangioma.[32] Less commonly, cerebral lesions include cerebral dysplasia, midline anomalies, and neuronal migration abnormalities (pachygyria, polymicrogyria, and heterotopic gray matter).[32,39-41] Associated midline defects include corpus callosum absence and pituitary lesions.[31,36] Cerebral vasculopathy of PHACE syndrome includes arterial anomalies and rare reports of venous abnormalities.[32,41] Primary arterial abnormalities can help distinguish PHACE from Sturge–Weber syndrome.[38] Common arterial abnormalities are arterial dysplasia (kinking, coiling, elongation), aneurysmal enlargement, arterial hypoplasia, agenesis, and non-congenital arterial stenosis/occlusion (Fig 4).[32] Besides, progressive arteriopathy and moyamoya-like vasculopathy were also reported in some patients.[32,42] Following the early appearance of facial hemangioma, neuroimaging detects regions of contrast enhancement that might overlie the hypoplastic cerebral or cerebellar areas.[43] Therefore, incorporating MRI sequences with gadolinium contrast demonstrates hemangioma intraorbital extension and enhancement, with delineation of dysplastic cerebral regions and the overlying pial enhancement.

Other Phakomatoses

Cowden Syndrome

Cowden syndrome (CS; MIM #158350), also called multiple hamartoma syndrome, is an autosomal dominant disorder characterized by multiple benign tumor growths (hamartomas) and increased risk of various malignancies, for example, breast, gastrointestinal, endometrial, and thyroid cancers. CS is very rare, with an incidence of approximately 1 in 200,000.[44]

Genetics: CS is caused by various mutations in a tumor suppressor gene called *PTEN* located on chromosome 10q22-23.[45] PTEN negatively regulates the PI3K/Akt/mTOR pathway, and loss of function of this protein promotes cell survival, growth, and migration. Other genes have also been implicated, including *KLLN, SDHB, SDHC, SDHD, PIK3CA*, and *AKT1*. Diagnosis is suggested by clinical criteria and confirmed by genetic testing. Lhermitte Duclos disease is characterized by dysplastic gangliocytoma of the cerebellum.[46] The term "COLD syndrome" describes the association of Cowden syndrome plus Lhermitte–Duclos disease.

Clinical presentation: CS patients present with a combination of major criteria (skin lesions, breast, endometrial, and thyroid cancer, GI hamartomas, dysplastic gangliocytoma of the cerebellum, or macrocephaly), and minor criteria (renal cell carcinoma, colon cancer, thyroid goiter or cancer, esophageal glycogenic acanthosis, vascular anomalies, lipomas, mental retardation, or testicular lipomatosis) in patients with or without known *PTEN* mutations.[47] Skin findings such as papular facial trichilemmomas are seen nearly in all patients and appear in the second decade of life. Mild macrocephaly presents in over 90% of the cases. Additionally, CS patients suffer from an increased risk of several types of cancer, most commonly breast and thyroid.

Neuroimaging: Brain imaging findings in CS patients include: (1) dysplastic gangliocytoma of the cerebellum, also known as Lhermitte-Duclos, seen in up to 50% of the patients; (2) Vascular malformations; (3) meningiomas (with variable frequency); and (4) increased white matter signal abnormalities and prominent perivascular spaces.[48] Lhermitte-Duclos lesions are characterized by a pattern of alternating hyper and hypointense bands (widened striated cerebellar folia, so-called tigroid appearance), with variable enhancement (Fig 5). Despite these lesions being hamartomas, they are classified as WHO grade I and can occasionally cause mass effect or obstructive hydrocephalus. These lesions could also present without other findings of CS and are well-known for post-resection recurrence. Although meningiomas are not hamartomatous and are not one of the CS criteria, some studies have reported increased prevalence in CS patients. One case series of 44 patients reporting 18% prevalence.[48] The genetic causes are unclear, with possible involvement of the *PTEN/AKT/PI3K* pathway.[49] Multiple developmental venous anomalies are observed in 30%-60%.[48] Other vascular anomalies include cavernous malformations (with and without DVAs) and

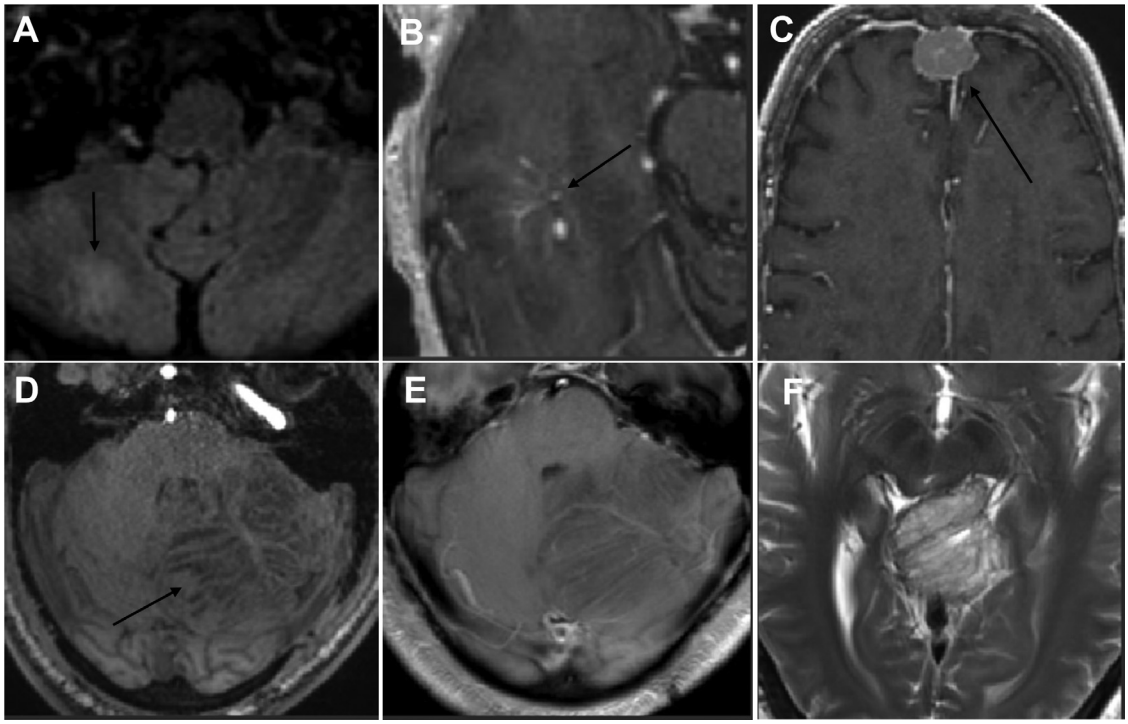

FIG 5. (5A-C) A 69-year-old with confirmed Cowden syndrome. (A) Axial FLAIR demonstrates a hyperintense lesion within the right cerebellar hemisphere (black arrow) most suggestive of a small dysplastic cerebellar gangliocytoma (Lhermitte-Duclos syndrome). (B) Axial post-contrast nonfat saturated T1WI shows a developmental venous anomaly (black arrow). (C) Axial post-contrast T1WI demonstrates a frontal meningioma (black arrow). (D-F) A 48-year-old patient Cowden-Lhermitte-Duclos (COLD) syndrome: (D) Axial T1WI shows a disorganized lesion with classical striated/tigroid appearance in the left cerebellar hemisphere (black arrow) consistent with Lhermitte-Duclos syndrome. (E) axial post-contrast T1WI demonstrate a similar appearance without evidence of significant enhancement. (F) Axial T2WI shows the lesion's classical striated appearance as it extends to involve the vermis and cause mass effect on the midbrain and cerebral aqueduct.

dural arteriovenous fistula. MRS could be used to confirm the benign hamartomatous nature of the Lhermitte-Duclos lesion by showing increased lactate level, decreased myo-inositol and N-acetyl-aspartate levels and decreased or normal choline level.[50,51]

Basal Nevus Syndrome

Basal Nevus syndrome (BNS; MIM #109400), also known as Gorlin–Goltz syndrome, or Nevoid Basal Cell Carcinoma Syndrome, is an autosomal dominant disease characterized by multiple basal cell carcinomas, skeletal abnormalities, jaw cysts, ectopic calcifications, and plantar or palmar pits.[52] BNS is a rare condition that affects 1 in 31,000 to 1 in 1,64,000 individuals. Conversely, less than 1% of those with basal cell carcinoma have BNS.

Genetics: BNS is most commonly caused by mutations in the *PTCH1* gene located on chromosome 9q22, which encodes for PTCH protein, a receptor for hedgehog protein in the SHH signaling pathway.[53] A two-hit model affecting the two *PTCH1* alleles has been proposed to explain BNS development. Additional mutations in the *SUFU* gene, located on chromosome 10q24-q25, and the *PTCH2* gene, located on chromosome 1p32, have also been described.

Clinical presentation: BNS patients usually present with basal cell carcinoma (BCC) on the face and trunk, which appears after puberty. Odontogenic keratocysts (OK, previously known as keratocystic odontogenic tumors) are also present. Additionally, patients suffer from an increased predisposition to other neoplasms. BNS diagnosis is based on clinical criteria[54]: major criteria (>2 BCC or BCC before 20 years, odontogenic keratocyst of the jaw, >3 cutaneous palmar or plantar pits, falcine calcification, rib anomalies, and affected 1st-degree relative) and minor criteria (childhood medulloblastoma, macrocephaly, orofacial malformation, skeletal anomalies, or ovarian or cardiac fibromas). Two major or one major plus two minor criteria suggest BNS diagnosis. Imaging workup should include neuroimaging and radiographs of chest, hands, and feet to evaluate for dysplasia.

Neuroimaging: The most common imaging finding in BNS is calcification of the falx cerebri apparent in CT scans. A case series of 82 patients shows that this finding is present in 80% of individuals older than 20 years.[55] Less frequently, calcification of the tentorium cerebellum, bridging of the sella, and abnormal frontal sinus aeration are also described in affected individuals.[55] Medulloblastoma in BNS is described as a solid and cystic mass in the posterior fossa. Head CT and MRI can also show OKs. OKs are benign cystic, usually multiple lesions involving the mandible or maxilla. These lesions are locally aggressive, with a high rate of recurrence after excision. On CT, OKs appear as expansile, cystic lesions with scalloped well-corticated borders, while on T1 MRI shows a high signal due to cholesterol and keratin content. Finally, imaging could also show asymmetric or dilated ventricles, cerebral atrophy, cavum septum pellucidum, dysgenesis, or agenesis of corpus callosum and meningiomas.[55] Examples of these imaging findings are presented in Figure 6.

Schwannomatosis

Schwannomatosis (MIM # 615670), also called Neurofibromatosis type 3 or congenital neurilemmomatosis, is an adult-onset disorder characterized by multiple schwannomas in various parts of the body.[56] This condition is very similar to NF-2 except for vestibular schwannomas (almost pathognomonic for NF-2), gliomas, or other lesions present with NF-2 and absent in schwannomatosis. It has a frequency of 1 in 40,000 to 1.7 million worldwide, with a peak incidence between the ages of 30 - 60 years.

Genetics: Schwannomatosis is primarily sporadic, but 15%-25% of conditions are inherited as autosomal dominant with incomplete penetrance.[56] Some cases are characterized by loss-of-function mutations in the *SMARCB1* gene (Schwannomatosis type 1) or *LZTR1* gene,

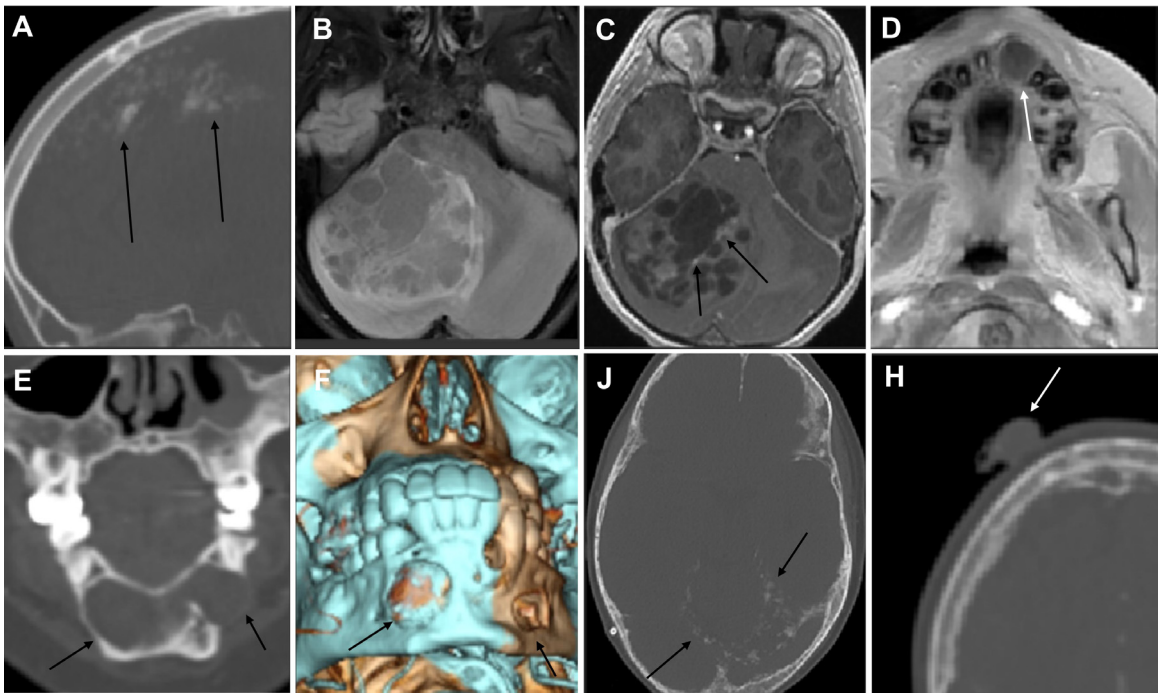

FIG 6. (A-D) A 8-year-old patient with Basal Nevus Syndrome. (A) Sagittal bone window non-contrast CT shows extensive lamellar calcifications of the falx cerebri (black arrows). (B) Axial FLAIR demonstrates a large posterior fossa solid and cystic mass confirmed to be medulloblastoma on resection. (C) Axial post-contrast T1WI shows faint foci of enhancement within the lesion black (black arrows). (D) Axial post-contrast nonfat saturated T1WI demonstrates a cyst within the maxilla (white arrow) consistent with an odontogenic keratocyst. (E-H) A 20-year-old patient with Basal nevus syndrome. (E) Coronal CT bone window demonstrates multiple mandibular cystic lesions (black arrows) consistent with Odontogenic Keratocysts. (F) 3D rendering of the facial bones demonstrates multiple Odontogenic Keratocysts. (J). An axial bone window shows lamellar calcifications involving the tentorial leaflets (black arrows). (H). Axial bone window CT shows a cutaneous nodule, confirmed to be a basal cell carcinoma. (Color version of figure is available online.)

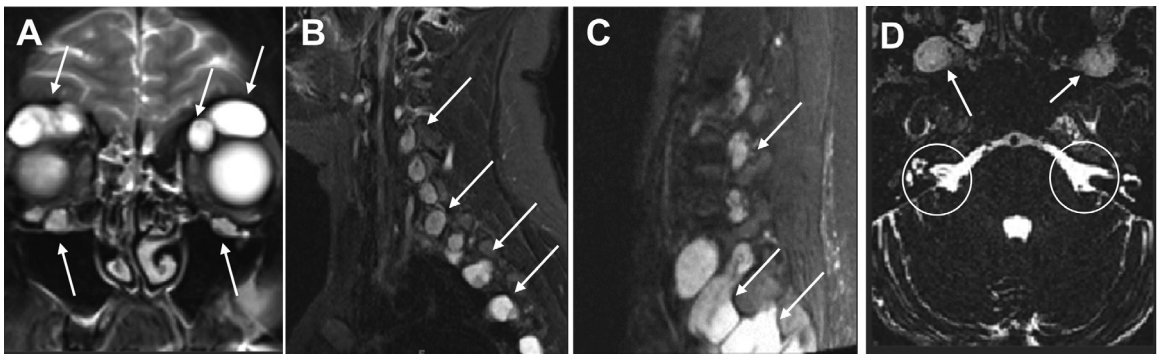

FIG 7. A 39-year-old with a confirmed history of Schwannomatosis. (A) coronal fat-saturated T2WI demonstrates bilateral orbital T2 hyperintense lesions along with the ophthalmic and maxillary trigeminal nerve branches divisions' distribution consistent with multiple schwannomas (white arrows). (B) Sagittal STIR cervical spine shows diffuse STIR hyperintense lesions consistent with schwannomas along all of the cervical and upper thoracic nerve roots (white arrows). (C) Sagittal STIR lumbar spine shows diffuse lumbar and sacral nerve roots schwannomas (white arrows). (D), axial heavily weighted T2 images show normal cerebellopontine angles/internal auditory canals (circles). Note ptyrgopalaltine fossa schwannomas (white arrows).

both genes located on chromosome 22q11 (Schwannomatosis type 2), and encode tumor suppressor proteins. Some cases have somatic mutations. The diagnosis is made based on the clinical presentation.

Clinical presentation: Patients with Schwannomatosis present with multiple schwannomas (> 2 intradermal) and do not meet diagnostic criteria for NF-2 (no ependymomas or meningiomas. The literature disagrees on whether vestibular schwannomas exclude the diagnosis. The onset of tumors ranged from the second to the sixth decade of life and appear in various parts of the body, including the spinal cord, chest wall, extremities, and subcutaneous regions.

Neuroimaging: Characteristic imaging finding in Schwannomatosis is multiple schwannomas with sparing of the vestibular nerves. MRI remains the imaging modality of choice. Schwannomas in imaging appear as well-defined, round or oval T2 hyperintense lesions located along the course of peripheral nerves with intense heterogeneous contrast enhancement with gadolinium-based contrast agents.[57] The most common nerves affected by these lesions include peripheral segments of the cranial nerves and spinal nerve roots. An example of the lesion is shown in Figure 7.

Progressive Facial Hemiatrophy

Progressive Facial Hemiatrophy (PFH), also called Parry Romberg Syndrome, is a rare craniofacial disorder characterized by slowly progressive atrophy of unilateral facial skin and soft tissues with a variable degree of severity and involvement.[58] About 20% of the patients show involvement of the limbs, trunk, as well, which could be either ipsi- or contralateral. The frequency of this condition is 1 in 250,000 with a possible female predominance.

Genetics: The genetic cause of this syndrome is unknown, and the diagnosis is made based on clinical presentation. A study of the

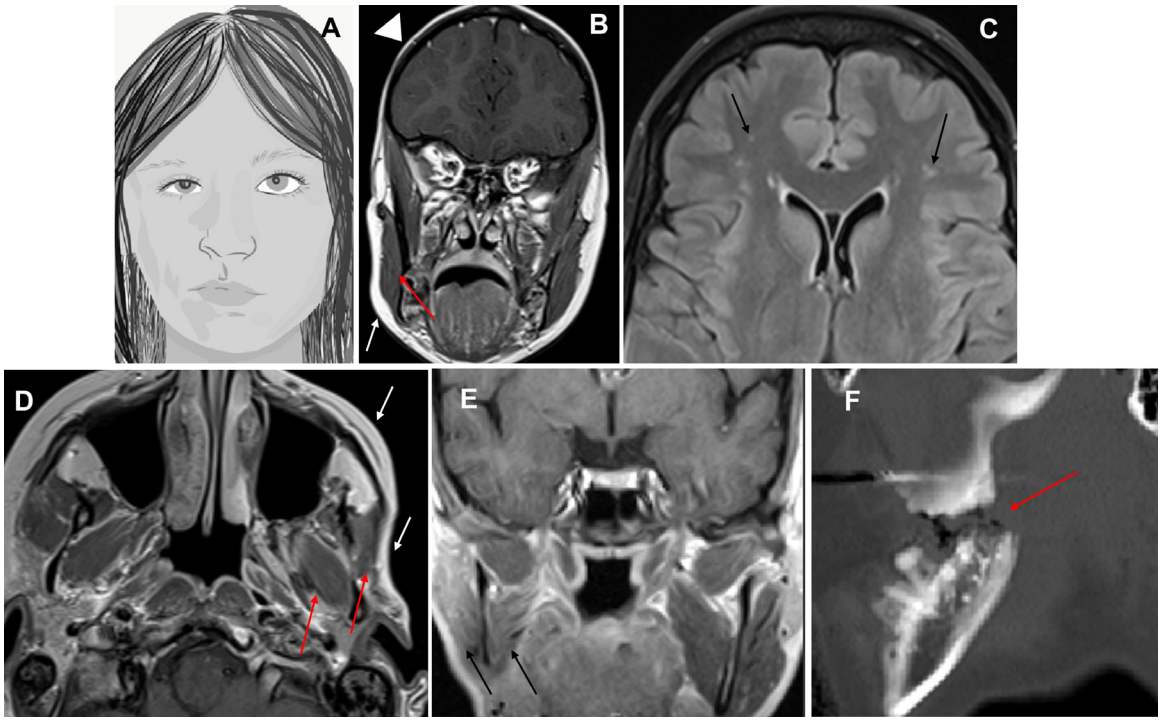

FIG 8. (A) Cartoon depicting classical findings of progressive facial hemiatrophy on the right with soft tissue loss and muscular bulk. (B) An 11-year-old with progressive facial hemiatrophy, Coronal nonfat saturated post-contrast T1WI shows right-sided hemiatrophy of the masseter muscle (red arrow), right facial subcutaneous fat (white arrow), and scalp (arrowhead) when compared to contralateral side. (C-D) A 37-year-old presenting with left-sided trigeminal neuralgia (C) Axial FLAIR demonstrates white matter hyperintense lesions (black arrows). (D) Axial post-contrast nonfat saturated T1WI demonstrates muscles of mastication (red arrows, pterygoid, and master muscles) and subcutaneous facial fatty atrophy (white arrows) when compared to contralateral site. (E-F) A 63-year-old presenting with right facial pain after chiropractor manipulation. (E) Coronal post-contrast nonfat saturated T1WI demonstrates fatty atrophy of the muscles of mastication (black arrows) compared to the contralateral face. (F) sagittal bone window CT shows right mandibular angle fracture (red arrow). (Color version of figure is available online.)

occurrence of PFH in one of a monozygotic twin pair also argued that this condition is unlikely to be genetic.[59]

Clinical presentation: Patients with PFH usually present in the second to fourth decade of life with complaints of the skin's abnormal texture and hyperpigmentation.[58] Physical examination usually reveals the extent and severity of involvement of the cutaneous and subcutaneous tissues of the cheek and forehead. Radiographic studies show bone involvement.

Neuroimaging: A classical imaging feature of PFH is unilateral atrophy, usually beginning in the maxillary region, with loss of soft tissue and muscular bulk. Loss of ocular fat may also cause enophthalmos. Unilateral intracranial vascular involvement, intracranial vascular dysplasia, intracranial calcifications, and white matter hyperintense lesion are also reported in cases of PFH.[60] Contralateral brain atrophy and sympathetic dysfunction have been also reported.[61] Mandibular fracture complications are not uncommon in these patients, given decrease in muscular bulk and bone dysplasia. An example of neuroradiological findings seen in PFH is shown in Figure 8.

Wyburn-Mason Syndrome

Wyburn-Mason syndrome (WMS) is a congenital neurocutaneous disease caused by developmental anomalies involving the primitive vascular mesoderm and the developing optic cup and anterior neural tube.[62] A hallmark of WMS is unilateral or bilateral multiple arteriovenous malformations (AVMs).[63,64] The anomalous vessels consist of arteries and veins without capillary beds resulting in direct arteriovenous communication.[64] These vessels can involve the visual pathway from the retina to the occipital cortex, hypothalamus, midbrain, basal ganglia, or cerebellum and may result in bleeding or thrombosis.[65] The exact prevalence of WMS in the general population is unknown. Around 100 cases have been reported in the literature.[62,64,65]

Genetics: No specific genetic cause of WMS has been identified. Furthermore, the specific underlying mechanisms for AVM development is not well characterized .

Clinical manifestations: The main features of WMS are ipsilateral intracranial AVMs, visual pathway, vascular anomalies, and facial nevi.[62] However, all three features are not always present. Ophthalmic manifestations may include monocular amblyopia, esotropia, glaucoma, or vision loss due to vitreous, intra-retinal, or macular bleeding.[64] In a literature review of 27 cases, all patients had eye-related findings, often due to retinal or orbital AVMs resulting in abnormal visual acuity, proptosis, pupillary defects, and optic atrophy.[62] Dermatological findings are uncommon and include angiomas of the face in the distribution of the trigeminal nerve, frontal or maxillary sinuses, or the pharynx. The neurological manifestations could include headache, hemiparesis, seizures, and retro-orbital pain.

Neuroimaging: MRI and CT help demonstrate the type, location, and extent of the brain and orbit vascular anomalies, including AVM. Cerebral angiography is usually needed to evaluate symptomatic patients and delineates the hemodynamics and the arterial supply of these lesions (Fig 9).[62] The most commonly affected sites are the orbit, particularly the optic nerve, followed by the thalamus, hypothalamus, optic chiasm, and suprasellar region. Brain lesions occur in the distribution of the optic tracts and optic radiations.[62] Brain damage close to vascular malformations can occur through compression of expanding AVM, ischemia or bleeding, or further complications like subarachnoid or intracerebral hemorrhages.[62,64] Occasionally, spontaneous obstruction of retinal AVM results in retinal bleed.[62]

Gomez-Lopez-Hernandez Syndrome

Gomez-Lopez-Hernández syndrome (GLHS; MIM #601853), also known as cerebello-trigeminal-dermal dysplasia, is a neurocutaneous syndrome with three primary features: partial scalp alopecia,

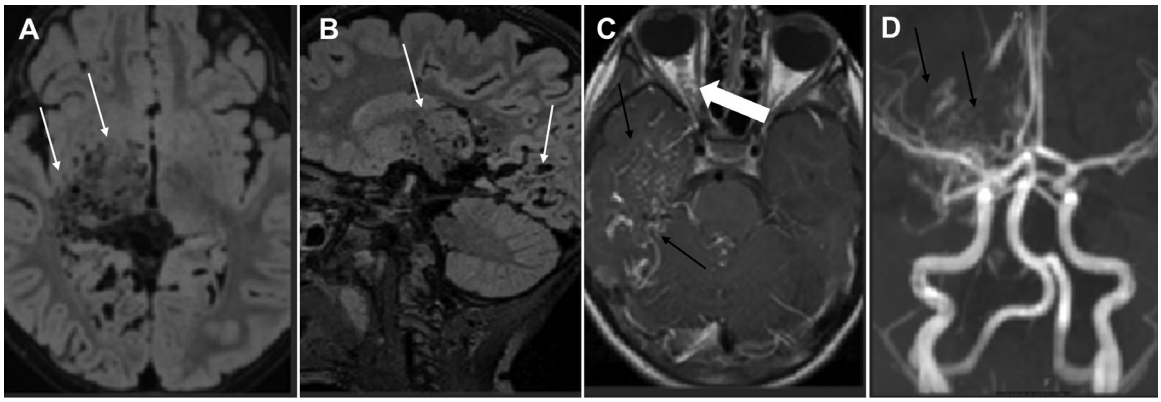

FIG 9. A 5-years-old Wyburn Mason syndrome, (A-B), axial and sagittal 3D FLAIR show multiple flow voids reflective of a large arteriovenous malformation (AVM) involving the thalamus and occipital lobes (white arrows). (C) Post-contrast T1WI further demonstrate the temporal lobe involvement (black arrow) and subtle extension to the orbit (white arrowhead) as noted by vascular congestion. (D) Axial time-of-flight MIP demonstrates extensive arterial supply from the anterior circulation (black arrows).

rhombencephalosynapsis, and trigeminal anesthesia. All 3 findings were reported in only 56% of patients.[66] The presence of the mentioned triad or the presence of rhombencephalosynapsis, with scalp alopecia and one major craniofacial manifestation, suggests a definitive GLHS.[67] Another study suggested GLHS should be considered if at least 2 of the following criteria are fulfilled: focal non-scarring alopecia, craniofacial anomalies, rhombencephalosynapsis, trigeminal anesthesia, or anatomic trigeminal nerve abnormalities.[68] Less than 100 cases are reported since its first description.[68,69]

Genetics: The cerebellar and cranial nerve abnormalities in GHLS occur as a consequence of an ectoderm developmental arrest.[70] The underlying etiology and genetic inheritance pattern of GHLS are still unclear.[68] However, consanguinity was reported in at least 3 cases, making autosomal recessive transmission a possibility.[66,71] No chromosomal abnormalities have been described to be related to GLHS. One of the potential recessive mutations that may be associated with GLHS was described to affect the gene encoding lysosomal acid phosphatase (ACP2), which maps in the human homologue to the location 11p11.2.[72]

Clinical presentation: Neurologic manifestations include hypotonia, motor delays, ataxia, intellectual disability, and stereotypical head movements.[66,67,73] Other reported craniofacial manifestations include brachycephaly, low-set ears, widely spaced eyes, strabismus, mid-face retrusion, turribrachycephaly, and craniosynostosis.[70,71,74] Individual cases report behavioral and psychiatric manifestations like self-mutilation, schizophrenia, and autism spectrum disorder.[69,73,75]

Neuroimaging: A classic feature of GLHS is Rhombencephalosynapsis. Brain MRI shows transversely oriented cerebellar folia with absent cerebellar vermis and fused cerebellar hemispheres, white matter, and dentate nuclei (Fig 10). Other imaging findings include ventriculomegaly/hydrocephalus, cerebellar hypoplasia, and trigeminal ganglia hypoplasia.[72,76] Supratentorial brain anomalies associated with rhombencephalosynapsis were also reported, including abnormal gyri, corpus callosal anomalies, large massa intermedia, thalamic fusion, and absent septum pellucidum.[72]

CHILD Syndrome

CHILD syndrome (MIM #308050) is characterized by unilateral skin inflammation with erythema and scaling and ipsilateral visceral and limb abnormalities, ranging from limb hypoplasia to complete limb absence.[77] These findings constitute the basis of the acronym; ***C***ongenital ***H***emidysplasia with ***I***chthyosiform erythroderma and ***L***imb ***D***efects.[78] The right side of the body is more likely involved than the left. CHILD syndrome can be misdiagnosed as inflammatory linear verrucous epidermal nevus, psoriasis, ichthyosis, or atypical erythrokeratodermia.[77] There are less than 50 genetically confirmed cases reported in the literature.[79]

Genetics: CHILD syndrome is an X-linked dominant disease related to mutations in the NAD(P)H steroid dehydrogenase-like protein gene (*NSDHL* gene). *NSDHL* gene is located in chromosome Xq28.[78] The affected protein is involved in cholesterol metabolism, and the defect will result in improper keratinocyte membrane and skin barrier, with consequent manifestations of CHILD syndrome.[80]

Clinical presentation: Skin involvement in CHILD often demonstrate a unique lateralization pattern with strict midline demarcation and a tendency to affect body folds. Bilateral symmetric skin lesions were also reported.[78,81] Other findings include ichthyosiform nevus, which manifests as lateralized plaques with narrow bands following Blaschko's lines or overlying waxy, thick scales, and verruciform xanthomas, which manifests as a fleshy, exophytic mass.[82] Limb and skeletal abnormalities may include scoliosis, hand or foot clefting, and epiphyseal stippling "chondrodysplasia punctata." Ipsilateral visceral abnormalities may involve vascular structures, lungs, kidneys, and brain.[77] These may include a single ventricle, mitral valve or septal defects, aortic coarctation, absent kidney, hydronephrosis, or absent lung. Neurologic abnormalities include ipsilateral hypoplasia of the cranial nerves or the cerebral hemisphere, mild intellectual impairment, hemiparesis, electroencephalographic abnormalities, sensorineural hearing loss, and decreased touch and heat sensation.[77]

Neuroimaging: Imaging studies play an essential role in evaluating musculoskeletal defects and detecting potential brain involvement. Commonly, these studies reveal the extent of skeletal and soft tissue abnormalities in the spine and limbs. Other less common findings include unilateral hypoplasia of the brain, dilated lateral ventricle, hypoplasia of the cranial nerves and the spinal cord, lumbar meningocele, and hydrocephalus.[83] An example of imaging findings observed in cases of CHILD syndrome is shown in Figure 11.

Proteus Syndrome

Proteus syndrome (PS; MIM #176920) is a highly variable, rare genetic disorder characterized by disproportionate asymmetric overgrowth of different tissue types, epidermal and connective tissue nevi, vascular malformation, and adipose tissue dysregulation.[84,85] Other features included intellectual disability and dysmorphic faces. PS is also called a partial gigantism-nevi-hemihypertrophy-macrocephaly syndrome, and it is considered part of the epidermal nevus syndrome group of disorders. PS is extremely rare, with a frequency of less than 1 in 1 million.

Genetics: PS is mainly sporadic and caused by a genetic variant of somatic mutation resulting in a regulatory growth gene called *AKT1*. This mutation results in gain-of-function in the *AKT1* gene, which regulates

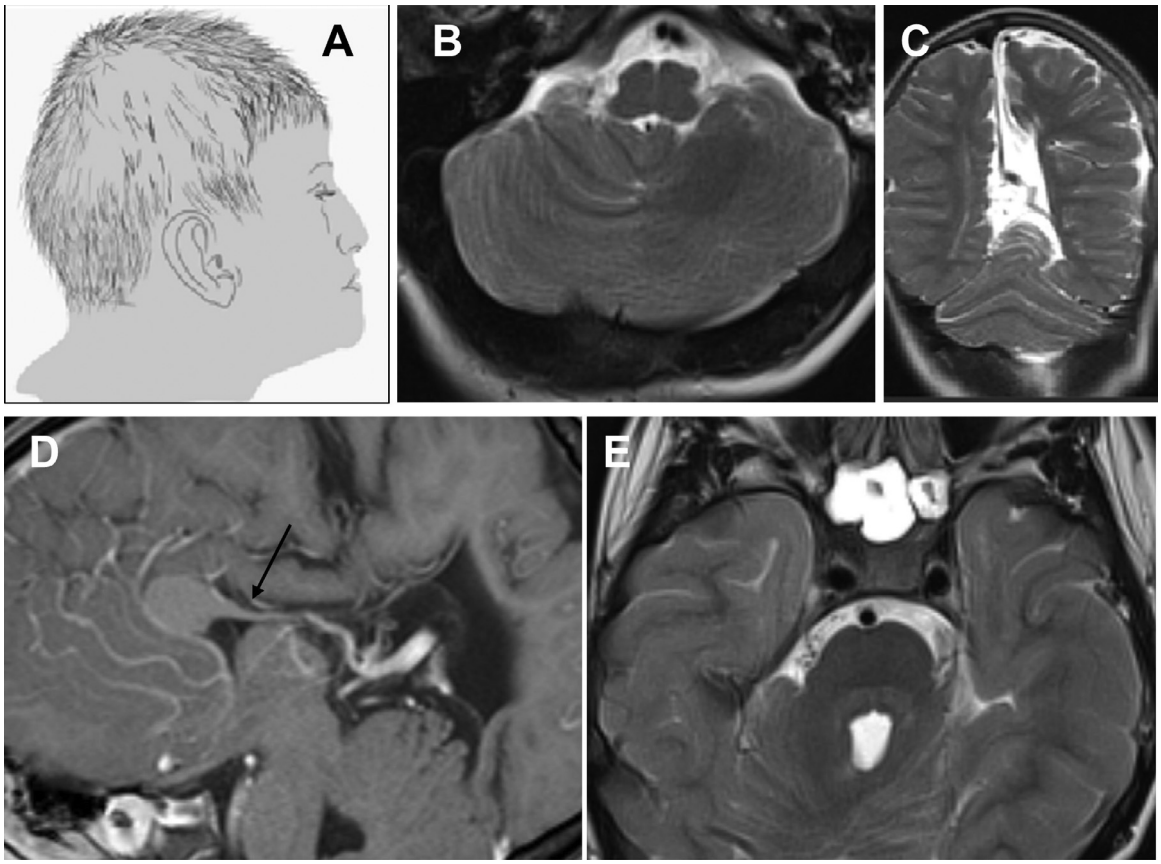

FIG 10. A 7-year-old patient with Gomez-Lopez-Hernandez Syndrome. (A) Cartoon depicting the classic alopecia and facial dysmorphic features in patients with GLHS. (B - C). Axial and coronal T2W images show cerebellar vermis hypoplasia with a fusion of the cerebellar hemispheres consistent with rhombencephalosynapsis (D) Sagittal post-contrast T1WI demonstrates corpus callosum dysgenesis (black arrow). (C) Axial T2W image shows Meckel's caves hypoplasia, possibly explaining the patient trigeminal anesthesia/paresthesia.

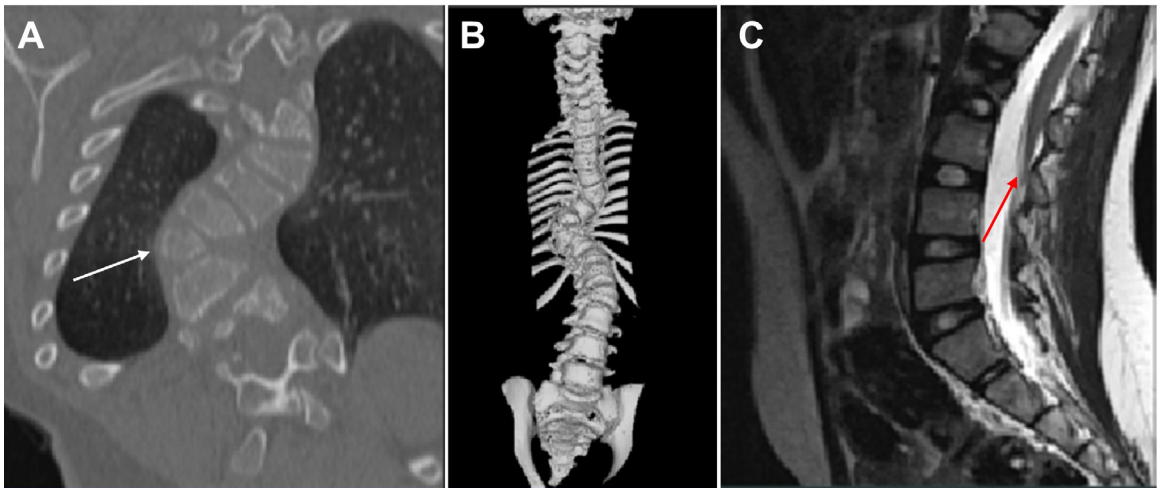

FIG 11. A 7 years old with CHILD Syndrome, (A) Coronal bone window CT demonstrates T9 hemivertebra (white arrow) with associated scoliosis and adjacent vertebral anomalies. (B) 3D rendered images further demonstrate the hemivertebra and scoliosis. (C) Lumbar spine sagittal T2W MRI shows borderline low lying conus medullaris at the level of L3 (red arrow). (Color version of figure is available online.)

cell proliferation and apoptosis. *AKT1* encodes for a kinase protein involved in regulating cell growth, proliferation, survival, differentiation, and cytoskeletal changes. Diagnosis is suspected upon clinical examination and imaging studies and confirmed with genetic testing.

Clinical presentation: Biesecker et al. suggested mandatory criteria for the diagnosis of PS that include mosaic distribution of lesions, sporadic occurrence, and progressive course.[84] Mosaic pattern of overgrowth primarily affects bones and skin. Progressive overgrowth of the cerebriform connective tissue nevus is pathognomonic for diagnosis.[86] PS is also associated with an increased risk of neoplasm and vascular malformations.

Neuroimaging: Classical imaging findings include asymmetric hemihypertrophy with bizarre irregular patterns of overgrowth, widespread lymphangitic or vascular malformations (Eg, arteriovenous

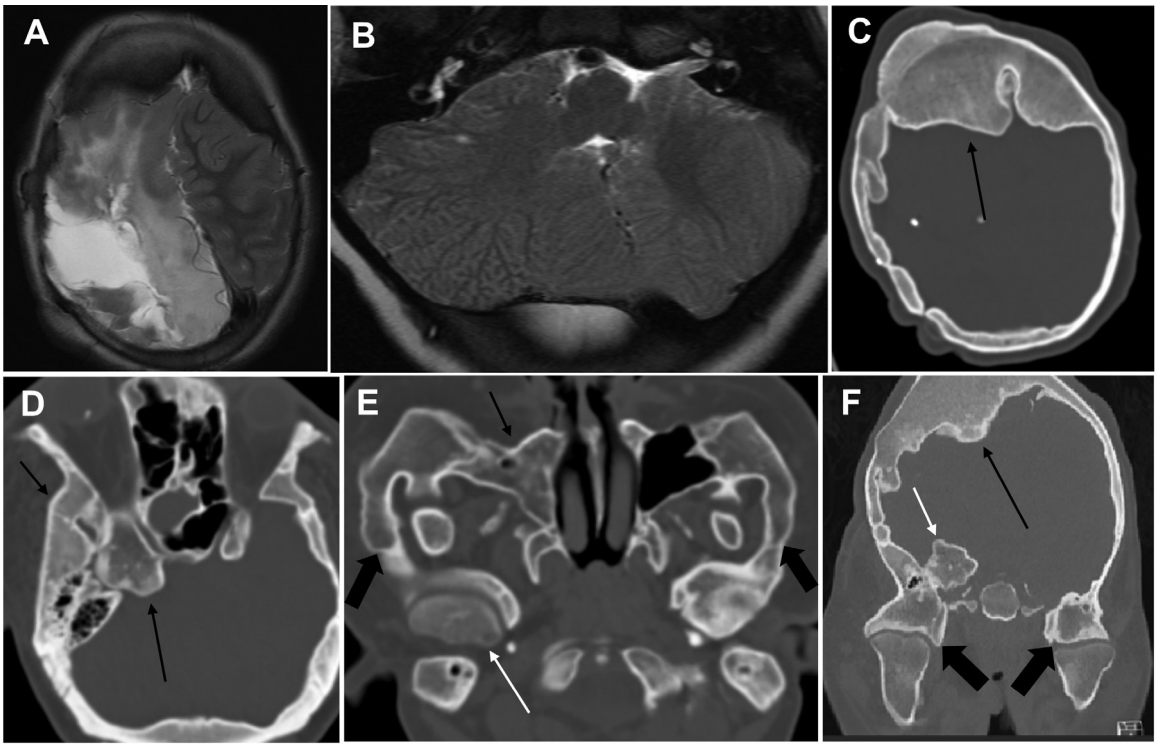

FIG 12. A patient with Proteus syndrome at different ages: Brain MRI at 8 years of age, CT scan at 19 years. (A) Axial T2W image demonstrates right cerebral hemisphere Hemimegalencephaly with extensive post-surgical changes of hemispherectomy and cortical/white matter T2 hyperintensity. (B) Axial T2W image at the level of the posterior fossa demonstrates hemihypertrophy of the right cerebellar hemisphere. (C). Axial bone window CT demonstrates marked calvarial expansion/overgrowth most prominent along the frontal bone (black arrow). (D) Axial bone window CT at the level of the orbits shows extensive right-sided squamosal temporal bone and sphenoid overgrowth (black arrows), resulting in multiple skull base foramina and orbital fissures narrowing. (E) Axial bone CT at the level of the maxillary sinus shows right maxillary sinus osseous overgrowth (black arrow), bilateral zygomatic arches overgrowth (black arrowheads), and right mandibular condyle overgrowth (white arrow). (F) Coronal bone window CT demonstrates calvarial expansion/overgrowth (black arrow), right sphenoid overgrowth (white arrow), and expansion/overgrowth of both temporomandibular joints (black arrowheads).

malformations), and hemimegalencephaly. Maxillary and mandibular deformations may occur secondary to overgrowth and subcutaneous fatty, fibrous, lymphangiomatous masses are common. Brain abnormalities are not common, but when present hemimegalencephaly and cortical migration defects are noted.[87,88] Additional imaging findings might include vertebral body defects, scoliosis, cranial exostosis, osteomas, osteochondromas, and enchondromas. Some of these imaging findings are shown in Figure 12.

Informed consent and patient details

The authors declare that this report does not contain any personal information that could lead to the identification of the patient(s).

References

1. Ruggieri M, Polizzi A, Paolo Marceca G, et al. Introduction to phacomatoses (neurocutaneous disorders) in childhood. Childs Nerv Syst 2020;36(10):2229–68.
2. Swarup MS, Gupta S, Singh S, et al. Phakomatoses: A pictorial review. Indian J Radiol Imaging 2020;30(2):195–205.
3. Nandigam K, Mechtler LL, Smirniotopoulos JG. Neuroimaging of neurocutaneous diseases. Neurol Clin 2014;32(1):159–92.
4. Kadonaga JN, Frieden IJ. Neurocutaneous melanosis: Definition and review of the literature. J Am Acad Dermatol 1991;24(5):747–55. Pt 1.
5. Castilla EE, da Graça Dutra M, Orioli-Parreiras IM. Epidemiology of congenital pigmented naevi: II. Risk factors. Br J Dermatol 1981;104(4):421–7.
6. Bett BJ. Large or multiple congenital melanocytic nevi: Occurrence of cutaneous melanoma in 1008 persons. J Am Acad Dermatol 2005;52(5):793–7.
7. Kinsler VA, Thomas AC, Ishida M, et al. Multiple congenital melanocytic nevi and neurocutaneous melanosis are caused by postzygotic mutations in codon 61 of NRAS. J Invest Dermatol 2013;133(9):2229–36.
8. Tannous ZS, Mihm Jr MS, Sober AJ, et al. Congenital melanocytic nevi: clinical and histopathologic features, risk of melanoma, and clinical management. J Am Acad Dermatol 2005;52(2):197–203.
9. Jakchairoongruang K, Khakoo Y, Beckwith M, et al. New insights into neurocutaneous melanosis. Pediatr Radiol 2018;48(12):1786–96.
10. Sung KS, Song YJ. Neurocutaneous melanosis in association with dandy-walker complex with extensive intracerebral and spinal cord involvement. J Korean Neurosurg Soc 2014;56(1):61–5.
11. Omar AT 2nd, Bagnas MAC, Del Rosario-Blasco KAR, et al. Shunt surgery for neurocutaneous melanosis with hydrocephalus: Case report and review of the literature. World Neurosurg 2018;120:583–9. e3.
12. Krengel S, Breuninger, H, Beckwith M, et al. Meeting report from the 2011 International Expert Meeting on Large Congenital Melanocytic Nevi and Neurocutaneous Melanocytosis. Tübingen Pigment Cell Melanoma Res 2011;24(4):E1–6.
13. Bolognia JL, Orlow SJ, Glick SA. Lines of Blaschko. J Am Acad Dermatol 1994;31(2):157–90. Pt 1quiz 190-2.
14. Fusco F, Paciolla M, Immacolata Conte M, et al. Incontinentia pigmenti: Report on data from 2000 to 2013. Orphanet J Rare Dis 2014;9:93.
15. Smahi A, Courtois G, Vabres P, et al. Genomic rearrangement in NEMO impairs NF-kappaB activation and is a cause of incontinentia pigmenti. The International Incontinentia Pigmenti (IP) Consortium. Nature 2000;405(6785):466–72.
16. Kawai M, Kato T, Tsutsumi M, et al. Molecular analysis of low-level mosaicism of the IKBKG mutation using the X Chromosome Inactivation pattern in Incontinentia Pigmenti. Mol Genet Genomic Med 2020;8(12):e1531.
17. Haque MN, Ohtsubo M, Nishina S, et al. Analysis of IKBKG/NEMO gene in five Japanese cases of incontinentia pigmenti with retinopathy: fine genomic assay of a rare male case with mosaicism. J Hum Genet 2021;66(2):205–14.
18. Emre S, Firat Y, Gungor S, et al. Incontinentia pigmenti: A case report and literature review. Turk J Pediatr 2009;51(2):190–4.
19. Soltirovska Salamon A, Lichtenbelt K, Cowan F M, et al. Clinical presentation and spectrum of neuroimaging findings in newborn infants with incontinentia pigmenti. Dev Med Child Neurol 2016;58(10):1076–84.
20. Pascual-Castroviejo I, Roche M C, Martinez Fernández V, et al. Incontinentia pigmenti: MR demonstration of brain changes. AJNR Am J Neuroradiol 1994;15(8):1521–7.
21. Lou H, Zhang L, Xiao W, et al. Nearly completely reversible brain abnormalities in a patient with incontinentia pigmenti. AJNR Am J Neuroradiol 2008;29(3):431–3.
22. Mulkey SB, Ramakrishnaiah RH, Balmakund TM. Cerebral Arteriopathy in a Newborn With Incontinentia Pigmenti. Pediatr Neurol 2016;54:76–81.
23. Swift M, Morrell D, Cromartie E, et al. The incidence and gene frequency of ataxia-telangiectasia in the United States. Am J Hum Genet 1986;39(5):573–83.
24. Zaki-Dizaji M, Mohammad Akrami S, Abolhassani H, et al. Ataxia telangiectasia syndrome: Moonlighting ATM. Expert Rev Clin Immunol 2017;13(12):1155–72.

25. Verhagen MM, Martin J, van Deuren M, et al. Neuropathology in classical and variant ataxia-telangiectasia. Neuropathology 2012;32(3):234–44.
26. Lin DD, Barker P B, Lederman H M, et al. Cerebral abnormalities in adults with ataxia-telangiectasia. AJNR Am J Neuroradiol 2014;35(1):119–23.
27. Ciemins JJ, Horowitz AL. Abnormal white matter signal in ataxia telangiectasia. AJNR Am J Neuroradiol 2000;21(8):1483–5.
28. Dineen RA, Blanchard C V, Pszczolkowski S, et al. Accumulation of Brain Hypointense Foci on Susceptibility-Weighted Imaging in Childhood Ataxia Telangiectasia. AJNR Am J Neuroradiol 2021;42(6):1144–50.
29. Wallis LI, Griffiths P D, Ritchie S J, et al. Proton spectroscopy and imaging at 3T in ataxia-telangiectasia. AJNR Am J Neuroradiol 2007;28(1):79–83.
30. Lin DD, Crawford T O, Lederman H M, et al. Proton MR spectroscopic imaging in ataxia-telangiectasia. Neuropediatrics 2006;37(4):241–6.
31. Frieden IJ, Reese V, Cohen D. PHACE Syndrome: The Association of Posterior Fossa Brain Malformations, Hemangiomas, Arterial Anomalies, Coarctation of the Aorta and Cardiac Defects, and Eye Abnormalities. Arch Dermatol 1996;132(3):307–11.
32. Heyer GL. PHACE(S) syndrome. Handb Clin Neurol 2015;132:169–83.
33. Kilcline C, Frieden IJ. Infantile hemangiomas: How common are they? A systematic review of the medical literature. Pediatr Dermatol 2008;25(2):168–73.
34. Metry DW, Haggstrom A N, Drolet B A, et al. A prospective study of PHACE syndrome in infantile hemangiomas: Demographic features, clinical findings, and complications. Am J Med Genet A 2006;140(9):975–86.
35. Haggstrom AN, Lammer E J, Schneider R A, et al. Patterns of infantile hemangiomas: New clues to hemangioma pathogenesis and embryonic facial development. Pediatrics 2006;117(3):698.
36. Bayer ML, Frommelt P C, Blei F, et al. Congenital cardiac, aortic arch, and vascular bed anomalies in PHACE Syndrome (from the International PHACE Syndrome Registry). Am J Cardiol 2013;112(12):1948–52.
37. Reese V, Frieden I J, Paller A S, et al. Association of facial hemangiomas with Dandy-Walker and other posterior fossa malformations. J Pediatr 1993;122(3):379–84.
38. Metry D, Heyer G, Hess C, et al. Consensus Statement on Diagnostic Criteria for PHACE Syndrome. Pediatrics 2009;124(5):1447.
39. Aeby A, Guerrini R, David P, et al. Facial hemangioma and cerebral corticovascular dysplasia. Neurology 2003;60(6):1030.
40. Grosso S, De Cosmo L, Bonifazi E, et al. Facial hemangioma and malformation of the cortical development: A broadening of the PHACE spectrum or a new entity? Am J Med Genet A 2004;124A(2):192–5.
41. Hess CP, Fullerton H J, Metry D W, et al. Cervical and intracranial arterial anomalies in 70 patients with PHACE Syndrome. Am J Neuroradiol 2010;31(10):1980.
42. Drolet BA, Dohil M, Golomb M R, et al. Early stroke and cerebral vasculopathy in children with facial hemangiomas and PHACE Association. Pediatrics 2006;117(3):959.
43. Heyer GL, Dowling M M, Licht D J, et al. The cerebral vasculopathy of PHACES syndrome. Stroke 2008;39(2):308–16.
44. Bubien V, Bonnet F, Brouste V, et al. High cumulative risks of cancer in patients with PTEN hamartoma tumour syndrome. J Med Genet 2013;50(4):255–63.
45. Blumenthal GM, Dennis PA. PTEN hamartoma tumor syndromes. Eur J Hum Genet 2008;16(11):1289–300.
46. Padberg GW, Schot D J, Vielvoye G J, et al. Lhermitte-Duclos disease and Cowden disease: A single phakomatosis. Ann Neurol 1991;29(5):517–23.
47. Pilarski R, Burt R, Kohlman W, et al. Cowden syndrome and the PTEN hamartoma tumor syndrome: Systematic review and revised diagnostic criteria. J Natl Cancer Inst 2013;105(21):1607–16.
48. Dhamija R, Weindling S M, Porter A B, et al. Neuroimaging abnormalities in patients with Cowden syndrome: Retrospective single-center study. Neurol Clin Pract 2018;8(3):207–13.
49. Yakubov E, Ghoochani A, Buslei R, et al. Hidden association of Cowden syndrome, PTEN mutation and meningioma frequency. Oncoscience 2016;3(5–6):149–55.
50. Klisch J, Juengling F, Spreer J, et al. Lhermitte-Duclos disease: Assessment with MR imaging, positron emission tomography, single-photon emission CT, and MR spectroscopy. AJNR Am J Neuroradiol 2001;22(5):824–30.
51. Anik Y, Anik I, Koc K, et al. MR Spectroscopy Findings in Lhermitte-Duclos Disease. A case report. Neuroradiol J 2007;20(3):278–81.
52. Koch CA, Chrousos G P, Chandra R, et al. Two-hit model for tumorigenesis of nevoid basal cell carcinoma (Gorlin) syndrome-associated hepatic mesenchymal tumor. Am J Med Genet 2002;109(1):74–6.
53. Johnson RL, Rothman, A L, Xie J, et al. Human homolog of patched, a candidate gene for the basal cell nevus syndrome. Science 1996;272(5268):1668–71.
54. Kimonis VE, Goldstein A M, Pastakia B, et al. Clinical manifestations in 105 persons with nevoid basal cell carcinoma syndrome. Am J Med Genet 1997;69(3):299–308.
55. Kimonis VE, Mehta S G, Digiovanna J J, et al. Radiological features in 82 patients with nevoid basal cell carcinoma (NBCC or Gorlin) syndrome. Genet Med 2004;6(6):495–502.
56. Piotrowski A, Xie J, Liu Y F, et al. Germline loss-of-function mutations in LZTR1 predispose to an inherited disorder of multiple schwannomas. Nat Genet 2014;46(2):182–7.
57. Koontz NA, Wiens A L, Agarwal A, et al. Schwannomatosis: The overlooked neurofibromatosis? AJR Am J Roentgenol 2013;200(6):W646–53.
58. Kaliyadan F, Biswas K, Dharmaratnam AD. Progressive facial hemiatrophy - a case series. Indian J Dermatol 2011;56(5):557–60.
59. Hulzebos CV, de Vries T W, Armbrust W, et al. Progressive facial hemiatrophy: A complex disorder not only affecting the face. A report in a monozygotic male twin pair. Acta Paediatr 2004;93(12):1665–9.
60. Taylor HM, Robinson R, Cox T. Progressive facial hemiatrophy: MRI appearances. Dev Med Child Neurol 1997;39(7):484–6.
61. Guo ZN, Zhang H, Zhou H, et al. Progressive facial hemiatrophy revisited: A role for sympathetic dysfunction. Arch Neurol 2011;68(9):1195–7.
62. Dayani PN, Sadun AA. A case report of Wyburn-Mason syndrome and review of the literature. Neuroradiology 2007;49(5):445–56.
63. Kim J, Kim O H, Suh J H, et al. Wyburn-Mason syndrome: An unusual presentation of bilateral orbital and unilateral brain arteriovenous malformations. Pediatr Radiol 1998;28(3):161.
64. Shyam K, Andrew D, Johny J. Child with Wyburn-Mason syndrome presenting with sudden onset of intracranial haemorrhage. BMJ Case Rep 2020;13(7):1.
65. Horkovicova K, Popov I, Tomcikova D, et al. The natural history of retinal vascular changes from infancy to adulthood in Wyburn-Mason Syndrome. Medicina (Kaunas, Lithuania) 2020;56(11):598.
66. Choudhary A, Minocha P, Sitaraman S. Gomez-Lopez-Hernández syndrome: First reported case from the Indian subcontinent. Intractable Rare Dis Res 2017;6(1):58–60.
67. Rush ET, Adam M P, Clark R D, et al. Four new patients with Gomez-Lopez-Hernandez syndrome and proposed diagnostic criteria. Am J Med Genet A 2013;161a(2):320–6.
68. Perrone E, Perez A P A, D'Almeida V, et al. Clinical and molecular evaluation of 13 Brazilian patients with Gomez-López-Hernández syndrome. Am J Med Genet A 2020;185(4):1047–58.
69. Kotetishvili B, Makashvili M, Okujava M, et al. Co-occurrence of Gomez-Lopez-Hernandez syndrome and Autism Spectrum Disorder: Case report with review of literature. Intractable Rare Dis Res 2018;7(3):191–5.
70. Gomez MR. Cerebellotrigeminal and focal dermal dysplasia: A newly recognized neurocutaneous syndrome. Brain Dev 1979;1(4):253–6.
71. de Mattos VF, Graziadio C, Machado Rosa R F, et al. Gómez-López-Hernández syndrome in a child born to consanguineous parents: new evidence for an autosomal-recessive pattern of inheritance? Pediatr Neurol 2014;50(6):612–5.
72. Tan TY, McGillivray G, Goergen S K, et al. Prenatal magnetic resonance imaging in Gomez-Lopez-Hernandez syndrome and review of the literature. Am J Med Genet A 2005;138(4):369–73.
73. Tuc E, Karaarslan E, Celik I, et al. Parieto-occipital alopecia in early infancy mandates cranial imaging. Clin Dysmorphol 2018;27(1):15–7.
74. López-Hernández A. Craniosynostosis , Ataxia, Trigeminal Anaesthesia and Parietal Alopecia with Pons-Vermis Fusion Anomaly (Atresia of the Fourth Ventricle). Report of two Cases. Neuropediatrics 1982;13(02):99–102.
75. Erzin G, Sücüllü Karadağ Y, Sözmen Cılız D, et al. Gómez-López-Hernández Syndrome: A case with Schizophrenia. Biol Psychiatry 2016;80(4):e25–7.
76. Perrone E, Burlin S, D'Almeida V, et al. Trigeminal ganglia hypoplasia as imaging clue for the diagnosis of Gómez-López-Hernández syndrome. Neurology 2020;96(11):1593–4.
77. Happle R. The group of epidermal nevus syndromes Part I. Well defined phenotypes. J Am Acad Dermatol 2010;63(1):1–22. quiz 23-4.
78. Bergqvist C, Abdallah B, Hasbani D, et al. CHILD syndrome: A modified pathogenesis-targeted therapeutic approach. Am J Med Genet A 2018;176(3):733–8.
79. Mi XB, Luo M, Guo L, et al. CHILD Syndrome: Case Report of a Chinese Patient and Literature Review of the NAD[P]H Steroid Dehydrogenase-Like Protein Gene Mutation. Pediatr Dermatol 2015;32(6):e277–82.
80. Seeger MA, Paller AS. The role of abnormalities in the distal pathway of cholesterol synthesis in the Congenital Hemidysplasia with Ichthyosiform erythroderma and Limb Defects (CHILD) syndrome. Biochim Biophys Acta 2014;1841(3):345–52.
81. König A, Happle R, Bornholdt D, et al. Mutations in the NSDHL gene, encoding a 3beta-hydroxysteroid dehydrogenase, cause CHILD syndrome. Am J Med Genet 2000;90(4):339–46.
82. Raychaudhury T, George R, Mandal K, et al. A novel X-chromosomal microdeletion encompassing congenital hemidysplasia with ichthyosiform erythroderma and limb defects. Pediatr Dermatol 2013;30(2):250–2.
83. Schmidt-Sidor B, Obersztyn E, Szymańska K, et al. Brain and cerebellar hemidysplasia in a case with ipsilateral body dysplasia and suspicion of CHILD syndrome. Folia Neuropathol 2008;46(3):232–7.
84. Biesecker LG, Happle R, Mulliken J B, et al. Proteus syndrome: diagnostic criteria, differential diagnosis, and patient evaluation. Am J Med Genet 1999;84(5):389–95.
85. Cohen MM Jr. Proteus syndrome review: Molecular, clinical, and pathologic features. Clin Genet 2014;85(2):111–9.
86. Beachkofsky TM, Sapp J C, Biesecker L G, et al. Progressive overgrowth of the cerebriform connective tissue nevus in patients with Proteus syndrome. J Am Acad Dermatol 2010;63(5):799–804.
87. DeLone DR, Brown WD, Gentry LR. Proteus syndrome: craniofacial and cerebral MRI. Neuroradiology 1999;41(11):840–3.
88. Griffiths PD, Welch R J, Gardner-Medwin D, et al. The radiological features of hemimegalencephaly including three cases associated with proteus syndrome. Neuropediatrics 1994;25(3):140–4.